

Processing and properties of a bioactive glass-ceramic reinforced with ductile silver particles

E. CLAXTON, B. A. TAYLOR, R. D. RAWLINGS

*Department of Materials, Imperial College of Science, Technology and Medicine,
Prince Consort Road, London SW7 2BP, UK
E-mail: r.rawlings@ic.ac.uk*

In order to overcome the problem of an adverse interfacial reaction which occurs when bioactive 'Apoceram' glass-ceramic is reinforced with titanium particles, we have investigated employing silver as the reinforcement. Composites reinforced with 10vol% silver were successfully produced by two routes, namely hot pressing and cold forming followed by sintering and crystallisation. There was no difference in the microstructure of the matrices other than the presence of large ($\sim 10 \mu\text{m}$) pores in the materials produced by the cold formed route. The matrices were free from microcracks and no reaction was observed between the matrix and the silver particles. The flexural strength and single edge notched bend toughness were determined at room temperature for the composites and the corresponding monolithic materials. Although the strength of cold formed monolithic material was poor compared with that produced via hot pressing, there was no difference in the mechanical properties of the composites produced by the two routes. It is therefore recommended that future development of the composites should concentrate on the less expensive cold-forming route. © 2002 Kluwer Academic Publishers

1. Introduction

Bioactive, or surface active, materials are designed to induce specific biological activity that results in the formation of a strong bond with the surrounding tissue [1]. Some specialised bioactive materials bond to soft tissue, but in most cases the desired biological reaction is one that results in a strong bond to bone. The bond strength can be sufficient for fixation of an implant in the bone without having to resort to mechanical methods such as cementing or screwing.

The first bioactive implant materials were glasses that were developed in the seventies by Hench and co-workers [2, 3]. These bioactive glasses are widely used but suffer from poor mechanical properties and, as a consequence, bioactive glass-ceramics with superior mechanical performance have been developed, e.g., Ceravital [4–6], AW glass-ceramic [7–9], Apoceram [10–12].

Apoceram is a bioactive glass-ceramic in the $\text{Na}_2\text{O}-\text{CaO}-\text{Al}_2\text{O}_3-\text{SiO}_2-\text{P}_2\text{O}_5$ system which has been developed at Imperial College. It has a fine microstructure consisting of two crystalline phases, wollastonite (CaSiO_3) and apatite [$\text{Ca}_5(\text{PO}_4)_3\text{OH,F}$], and some residual glass. Although the mechanical performance of Apoceram and other bioactive glass-ceramics is superior to that of bioactive glasses, further improvements are required for critical high stress applications. Consequently interest has developed in reinforcing bioactive glasses [e.g., 13–15] and glass-ceramics [e.g., 16–24].

The most commonly employed reinforcements have been metals.

Titanium has been employed for ductile particle reinforcement of Apoceram [21–24]. Ti was chosen because it is an inert, biocompatible material that is widely used as an implant material. However, during composite fabrication at elevated temperatures, the Ti reinforcement reacts with the SiO_2 in the Apoceram matrix to form a brittle reaction layer of Ti_5Si_3 [21]. Later it was shown that the extent of the interfacial reaction could be restricted by either adjustment of the composition of the Apoceram matrix by the addition of sodium silicate to reduce the sintering and crystallisation temperatures [22, 23] or by depositing diffusion barrier coatings onto the Ti particles prior to their introduction into the Apoceram matrix [24]. An alternative approach is to replace titanium with another biocompatible metal, such as silver, that may not react to the same extent with the matrix. The processing, structure and mechanical properties of silver reinforced Apoceram are reported in this paper.

2. Experimental procedures

2.1. Glass and reinforcement powders

The parent glass (CP1) was made from the raw materials and batch components given in Table I. With the exception of $\text{Na}_2\text{CO}_3 \cdot 10\text{H}_2\text{O}$, which was stored in a moist atmosphere to prevent efflorescence, all raw

TABLE I Raw materials and batch components for the production of Apoceram of the composition CP1

Raw material	Amount in batch (g)	Batch component
Sodium carbonate decahydrate	20.79	Na ₂ O(H ₂ O,CO ₂)
Calcium carbonate	36.43	CaO
Alumina	6.5	Al ₂ O ₃
Silica	51	SiO ₂
Calcium orthophosphate	15.5	CaO, P ₂ O ₅
Calcium Fluoride	2.79	CaO, F

materials were dried for 24 hours (at 1000°C for alumina and silica and 150°C for all other materials) before weighing in order to minimise errors associated with hydration. Na₂CO₃ · 10H₂O was in the form of small crystals and was ground prior to mixing with the dried powders in a pharmaceutical three-directional tumbling mixer for one hour.

The homogeneously mixed powder was placed in a platinum crucible, the temperature was raised to 1400°C, held for 3 hrs and then increased to 1500°C. Finally the melt was quenched into iced water, result-

ing in the formation of large glass fragments. The glass fragments were subsequently powdered using a tungsten carbide Tema mill and the resulting powder sieved to less than 38 μm. A typical particle size distribution, as determined using a Malvern Mastersizer laser diffraction analyser, is given in Fig. 1a.

An addition of 2.5 wt% sodium silicate was made to some of the glass powder. The sodium silicate was added in an aqueous form known as water glass; the 2.5 wt% refers to the mass of the equivalent dry sodium silicate and not to the amount of water glass. There was a negligible change in the particle size distribution as a result of adding the water glass (Fig. 1b). This powder is designated as CP1 : 2.5ss.

Silver of particle size ~50 μm and silver oxide were used for reinforcement; the latter decomposes to silver during composite fabrication. Both these powders were found to contain some agglomerates as demonstrated by the bi-modal particle size distributions (Fig. 1c and d). The agglomeration was most marked for the Ag₂O and hence the powder was passed through a 38 μm sieve prior to use.

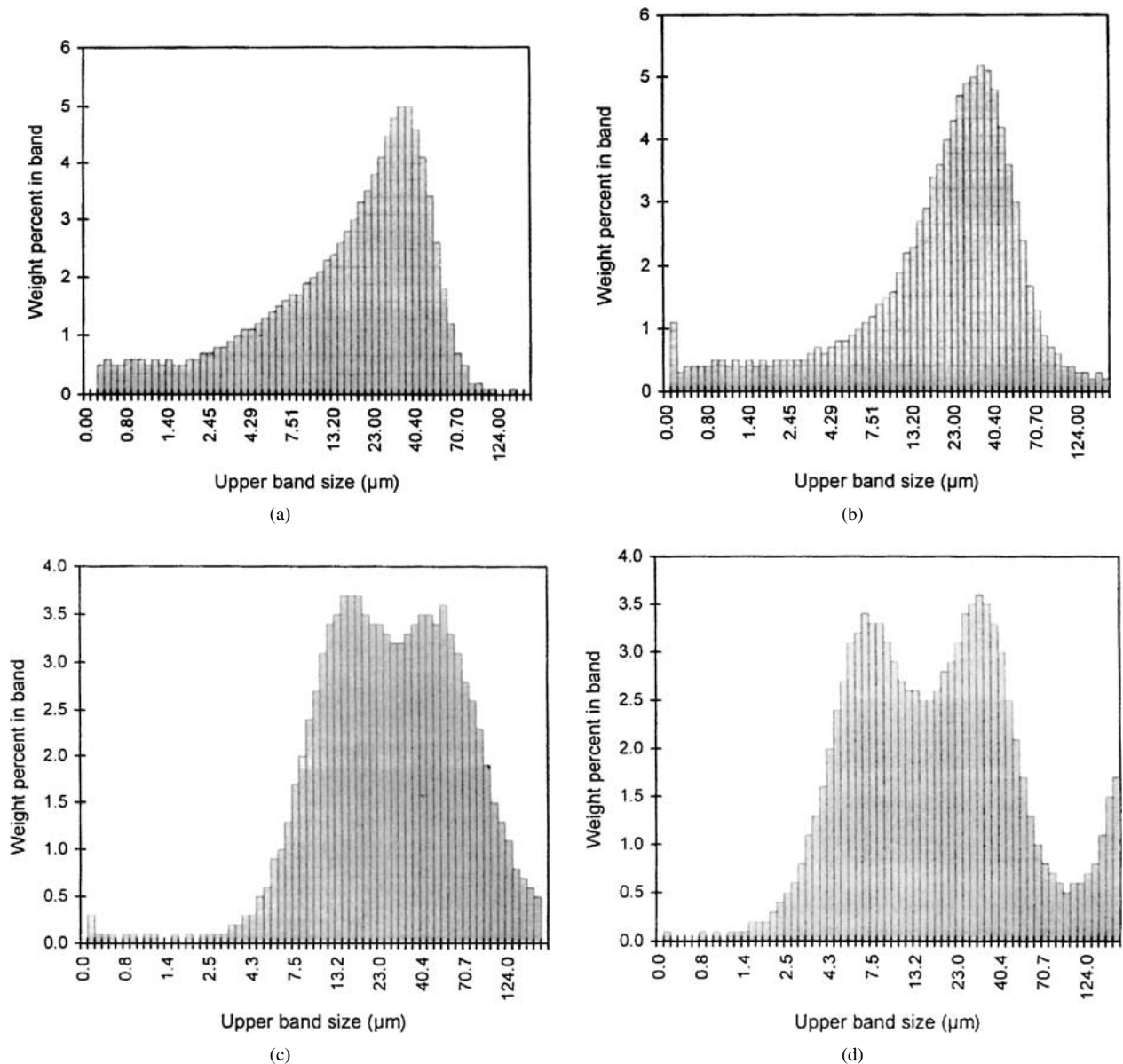


Figure 1 Particle size distribution of the powders: (a) CP1 glass (b) CP1 : 2.5ss glass (c) silver and (d) silver oxide.

TABLE II Composites fabricated and their designations (hp = hot pressed, cf, s & c = cold formed, sintered and crystallised)

Apoceram composite	Process	Temperature °C	Sample
CP1 reinforced with 20vol%silver	hp	1000	CP1-20/1000
CP1 reinforced with 10vol%silver	hp	1000	CP1-10/1000
CP1 reinforced with 10vol%silver	hp	950	CP1-10/950
CP1 : 2.5ss reinforced with 10vol%silver	hp	750/T; T = 850 to 925	CP1 : 2.5ss/T
CP1 : 2.5ss reinforced with 10vol%silver	cf, s & c	800/875	CP1 : 2.5ss/875
CP1 : 2.5ss reinforced with 10vol%silver via Ag ₂ O	cf, s & c	800/875	CP1 : 2.5ssAg ₂ O/8

2.2. Composite fabrication

A range of composites were produced by hot pressing or by cold pressing followed by a sintering and crystallisation heat treatment. In the former process, the required mixture of CPI or CP1 : 2.5ss, and Ag or Ag₂O (as given in Table II) was hot pressed in vacuum (10⁻⁴ torr) under a die pressure of 13 MPa. Most composites had 10 vol%Ag reinforcement and when Ag₂O was used, the addition was such to give 10vol%Ag. For CP1 the hot pressing was carried out at a one temperature whereas for CP1 : 2.5ss a two stage hot pressing procedure was followed; the lower hot pressing temperature (30 minutes at 750°C and 730°C for Ag and Ag₂O, respectively) facilitated sintering and the higher temperature (850°C to 925°C) was required for crystallisation. The samples were in the form of discs of nominal dimensions of 38 mm diameter and 5 mm thick.

The cold forming route consisted of cold uniaxial pressing to 100 MPa, isostatic cold pressing, with a pressure of 300 MPa, followed by 3 hours at 1000°C for CP1 and a two stage heat treatment of sintering for 2 hours at 800°C then a 2 hour crystallisation treatment at 875°C for CP1 : 2.5ss. The nominal dimensions of the samples were 3 mm × 5 mm × 30 mm. Monolithic samples were also prepared by the two processing routes for comparison purposes.

2.3. Structural characterisation

X-ray diffraction (XRD) was used to determine the nature and proportions of the crystalline phases in the composites. Solid samples were scanned at 1°/minute in a Philips diffractometer employing Cu K_α radiation. Magnesium oxide in the form of periclase was used as an internal standard.

Scanning electron microscopy (SEM), in both secondary and backscattered modes, was used to study the microstructures.

The amount of porosity present in the composites was determined from a comparison of the theoretical density, calculated from the law of mixtures, and experimental density as measured by Archimedes' method.

2.4. Mechanical testing

The hot-pressed discs were lapped using 1400 grit alumina powder to produce parallel faces and cut into bars using a high speed diamond saw. The ratio of the bar dimensions for three-point bending tests was 2.5 : 5 : 20 (*B* : *W* : *S*), where *B* and *W* (~5 mm) are the width and thickness of the specimen respectively, and *S* is the distance (20 mm) between the supports. Prior to testing the tensile face of the test bars was polished to a 1 μm

Al₂O₃ grit finish. Bars for strength testing also had the longitudinal edges of the tensile face bevelled using 1200 grit SiC paper to remove any flaws that may have been introduced during cutting. Bars for fracture toughness testing were also notched to a depth of 0.17*W* on the tensile side using a silicon disc with 400 grit. The notch had a nominal thickness of 0.15 mm.

The room temperature flexural strength was determined using a three-point bend test rig on a Nene M3000/64K testing rig at a cross-head speed of 1 mm/min. The flexural strength was calculated using the equation:

$$\sigma_f = 3Ps/2BW^2 \quad (1)$$

where σ_f is flexural strength, *P* is load at break, and *B* and *W* have been defined earlier.

The plain strain fracture toughness was determined using the single edge notch bend (SENB) test in three-point bending. The notch depth was measured for each sample using a calibrated optical microscope. The plane strain fracture toughness (*K_{IC}*) was calculated from experimental data using the equation:

$$K_{IC} = Y(3Ps/2BW^2)a^{0.5} \quad (2)$$

where *a* is notch depth and *Y* is a compliance factor which is given by:

$$Y = \{1.99 - a/W(1 - a/W)(2.15 - 3.39a/W) + 2.7(a/W)^2\} / \{(1 + 2a/W)(1 - a/W)^{1.5}\} \quad (3)$$

and is valid for 0 < *a*/*W* < 1 and for *s*/*W* = 4 [25].

Vickers hardness tests were carried out on polished surfaces in order to study the crack paths of the small cracks that emanated from the corners of the indentations.

3. Results and discussion

3.1. Structure of composites

3.1.1. Hot pressed

The only composite that was unsatisfactory and therefore not examined and tested was that containing 20vol%Ag and produced by hot pressing at 1000°C (CP1-20/1000). The hot press temperature was approximately 40°C above the melting point of silver (962°C) and so the metal was fluid and, as under pressure, flowed, linked-up and deposited on the surface of the composite. The same problem was not encountered with the composite containing 10vol%Ag and fabricated under the same hot pressing conditions, presumably because the silver content was insufficient for the

liquid metal regions to link-up and hence form a continuous route for flow to the surface. A similar change in the difficulty of manufacture by hot pressing with increasing vol% metal has been observed with aluminium reinforced 'Silceram' glass-ceramic [26]. In the case of the composites with a matrix of CP1 : 2.5ss, the problem does not arise as the lower sintering and crystallisation temperatures [22, 23] enabled a hot press temperature of less than the melting point of silver to be employed.

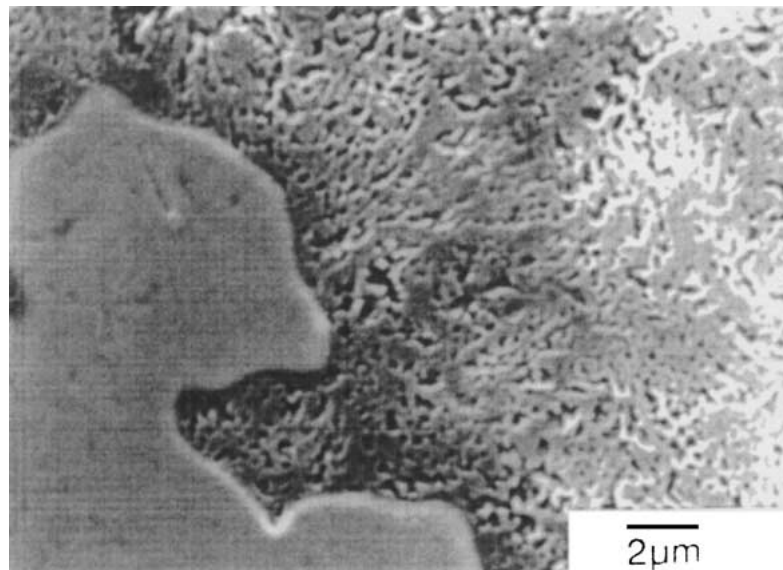
The size of the silver reinforcement particles in the composites produced from the silver oxide precursor was variable. Clearly there had been some agglomeration of the silver oxide on mixing with the glass, but nevertheless the silver particle size was still smaller when the oxide precursor was used. Agglomeration was less marked when silver was mixed with the glass to produce the composite.

No evidence of a matrix-silver interfacial reaction, or the presence of porosity at the interface, was found in the scanning electron microscopy examination of these composites (Fig. 2). This is in marked contrast to the situation when titanium is used for the reinforcement

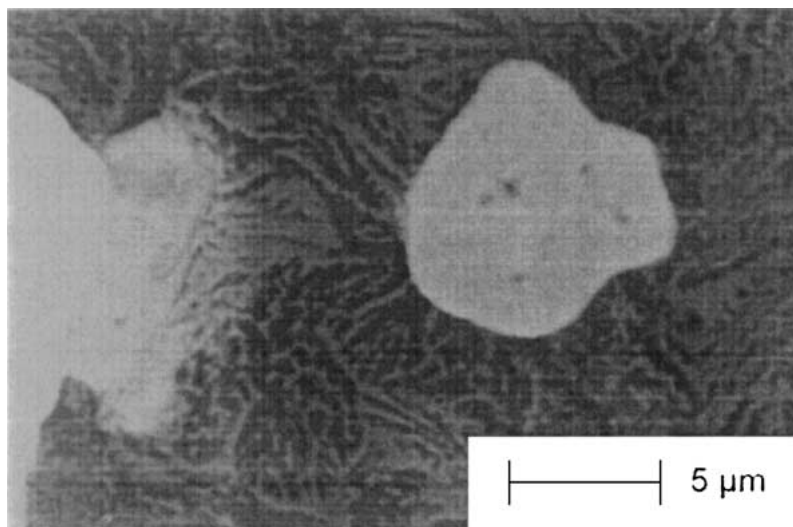
[21–24]. Silver has a coefficient of expansion that is almost twice that of the glass-ceramic matrix, therefore there is a propensity for the metal reinforcement to debond and pull away from the matrix thus forming pseudopores. Since pseudopores were not observed it is concluded that there is strong interfacial bonding. The differences in the coefficient of expansion of the components would also have lead to a tensile radial stress in the surrounding matrix but these were not sufficient to produce circumferential cracking. Thermal stress induced microcracking will only occur if the particles are above a critical diameter, D_c , given by [27, 28]:

$$D_c = \pi \frac{K_{Ic(m)}^2}{2P_o^2} \quad (4)$$

where $K_{Ic(m)}$ is the fracture toughness of the matrix and P_o is the thermally induced hydrostatic pressure on the particle, which for a spherical particle may be calculated using Selsing's equation [29]. Using Selsing's equation and assuming the relevant temperature change was that for cooling from the glass transition temperature of the matrix to room



(a)



(b)

Figure 2 Scanning electron images of hot pressed composites: (a) CP1-10/1000 (backscattered electron image) (b) CP1 : 2.5ss10/900 (secondary electron image).

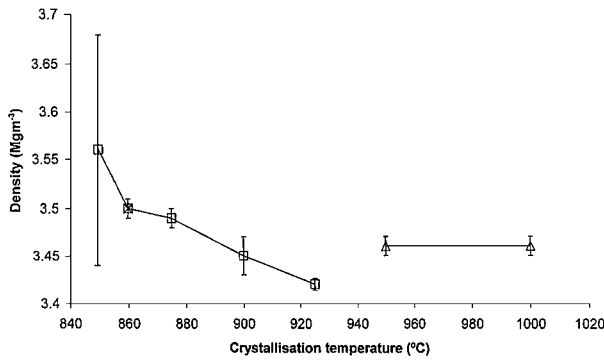


Figure 3 Variation in density of composites reinforced with 10vol%silver with final hot press (crystallisation) temperature (□ CP1:2.5ss with silver powder, △ CP1 with silver powder, × CP1:2.5ss with Ag₂O powder).

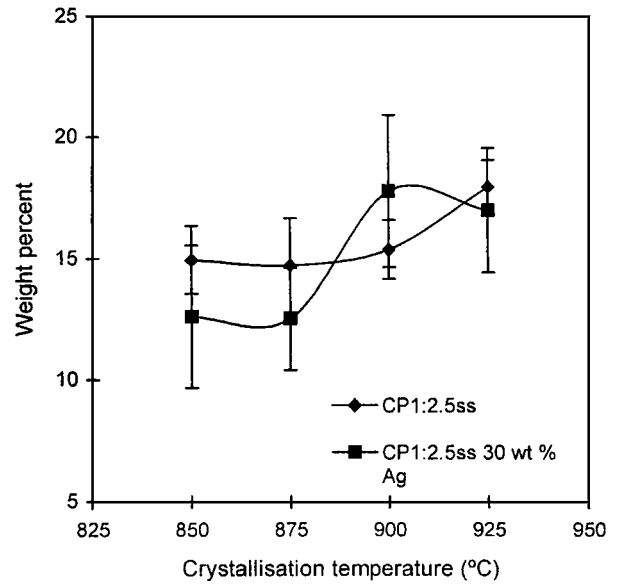
temperature, P_o was calculated to be around 650 MPa. Substituting this value for P_o into Equation 4 yielded a critical diameter of $\sim 10 \mu\text{m}$. Bearing in mind that the particle size distributions presented in Fig. 1 are in terms of weight percentage, it is clear that most of the silver particles in the powder were below the critical size of $10 \mu\text{m}$. Although some agglomeration of the silver particles did take place during processing this was not to the extent that reinforcement particles of significantly greater size than $10 \mu\text{m}$ were a common feature of the microstructure, hence matrix microcracking did not occur.

All hot pressed samples appeared fully dense except the AP:2.5ss matrix composites pressed at 900°C (AP:2.5ss/900) and 925°C (AP:2.5ss/925) which contained a small amount of porosity. This microstructural observation was confirmed by the density measurements (Fig. 3); samples AP:2.5ss/900 and AP:2.5ss/925 had the lowest densities. The density of the composites was similar irrespective of whether silver or its oxide was used in the production of the composite.

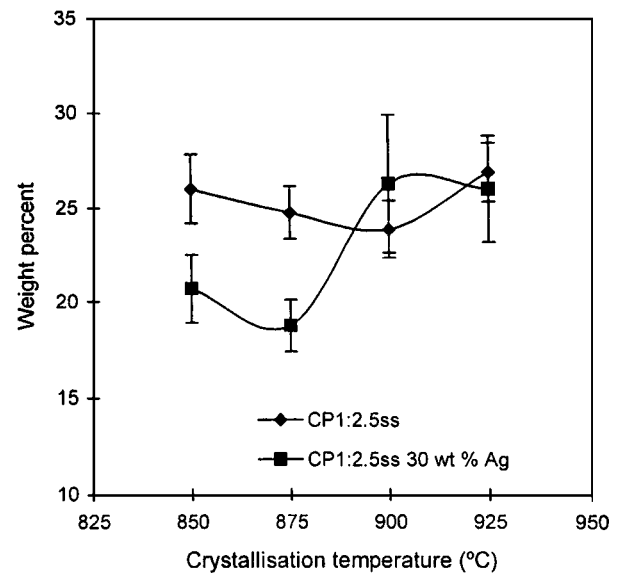
The microstructure of the monolithic materials and the CP1 and CP1:2.5ss matrices were similar consisting of fine crystals and some residual glass. X-ray diffraction identified the crystalline phases as hydroxyapatite, fluorapatite, parawollastonite and cyclowollastonite. Silver was, of course, also present in the x-ray patterns from the composites but no peaks were left unidentified unlike in the previous work on titanium-reinforced Apoceram. The amounts of apatite and wollastonite in monolithic CP1:2.5ss materials and in the matrices of their composite counterparts as a function of the final hot press (crystallisation) temperature are given in Fig. 4. It is concluded that, within the confidence limits of the technique, there is no evidence of a marked difference in the crystalline content of the monolithic materials and in the matrices. The total crystalline content is only about 40%; a reasonable proportion of glass is essential as it has been established that the bioactivity of glass-ceramics is associated with the residual glass [30].

3.1.2. Cold formed

The microstructures of the cold formed, sintered and crystallised composites were the same as described pre-



(a)



(b)

Figure 4 Crystalline content, as determined by x-ray diffraction, of hot pressed CP1:2.5ss monolithic materials and CP1:2.5ss matrices of composites as a function of the final hot press (crystallisation) temperature: (a) apatite (b) wollastonite.

viously for the hot pressed materials except for the presence of pores, many of which were $10 \mu\text{m}$ in size. Consequently the density of the cold formed monolithic and composite materials was about 3% less than that for the corresponding hot pressed materials.

3.2. Mechanical properties

The mechanical properties of the hot pressed monolithic material varied with the final hot press (crystallisation) temperature; the variations in strength and toughness being 106–160 MPa and 1.43–1.60 MPam^{1/2}, respectively over the temperature range used in this investigation. Therefore to facilitate comparison of the effect of the silver reinforcement on properties as a function of processing temperature, all composite mechanical property data are normalised to the values for the monolithic material produced under the same conditions.

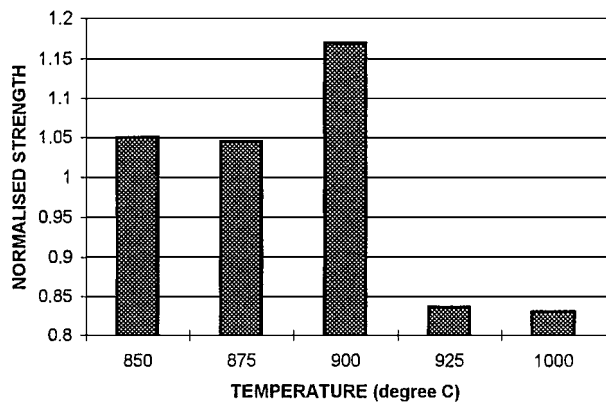


Figure 5 The strength of the hot pressed 10vol%Ag composites normalised to the strength of their monolithic counterparts as a function of the final hot press (crystallisation) temperature. 1000°C result is for CP1-10/1000, all other results are for the CP1 : 2.5ss/T series.

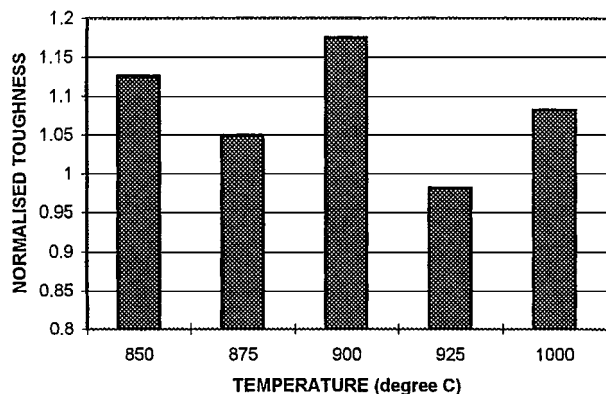


Figure 6 The fracture toughness of the hot pressed 10vol%Ag composites normalised to the strength of their monolithic counterparts as a function of the final hot press (crystallisation) temperature. 1000°C result is for CP1-10/1000, all other results are for the CP1 : 2.5ss/T series.

The normalised strength was greater than unity for processing temperatures 850–900°C inclusive but fell below unity at higher temperatures (Fig. 5). This was a consequence of the strength of the monolithic materials being greater the higher the processing temperature rather than the strength of the composites falling with increasing temperature. In fact the strength of the composites varied little over the temperature range investigated which means that temperature control during processing on an industrial scale would not be critical. No significant difference was observed between the strengths of the composites produced with silver and silver oxide.

The normalised toughness was greater than unity at all temperatures other than 925°C where the value was very close to unity (Fig. 6). In the case of toughness of the monolithic materials, the change with processing temperature was less marked than for strength; a similar small temperature dependence of toughness was observed for the composites. The toughening increment ΔG associated with ductile metal reinforcement particles of radius r is, according to Ashby, Blunt and Bannister [31], given by:

$$\Delta G = C A_f \sigma_y r \quad (5)$$

where A_f and σ_y are the areal fraction and the yield stress of the reinforcement respectively, and C is a con-

stant known as the constraint factor. A large increase in fracture toughness due to the silver particles was not observed in the present work, however as it has been demonstrated that composites can be processed without melting the silver it should be possible to enhance the toughness increment by increasing the volume fraction of ductile reinforcement. Equation 5 also indicates that ΔG is directly proportional to the yield stress. The yield stress of silver is low and, provided biocompatibility is not impaired, it would be preferable to use a strong silver alloy for the reinforcement.

The normalised toughness of the composites produced with silver and silver oxide, which resulted in smaller silver particles, were 1.09 and 0.86 respectively; this is consistent with Equation 5 which gives toughness to be directly proportional to the size of the reinforcing particles. There appears to be no benefit in using the oxide in composite production as it has a tendency to agglomerate and is more expensive than the element.

As discussed earlier the difference in expansion coefficients leads to hoop tension in the matrix around a silver particle and consequently a propagating crack will be attracted towards the particle. Similarly the fact that the Young's modulus of silver (80 GPa) is less than that of the matrix (94 GPa) means that a propagating crack would tend to be deflected towards the particles. There are then three possibilities once the crack reaches a particle: (i) the crack propagates through the particle with little plastic deformation, (ii) a limited amount of debonding occurs and the particle deforms, and (iii) the crack is deflected along a weak matrix-reinforcement interface. Possibility (ii), which requires an intermediate interfacial strength and a ductile particle, is the most desirable for good mechanical performance and was commonly observed in the present work (Fig. 7). Fractography revealed partially debonded silver particles that had been heavily deformed and fractured standing proud of the matrix (Fig. 8). The fracture characteristics indicate crack bridging with extensive plastic deformation of the silver particles and thus the composites are expected to exhibit an increasing toughness with crack length, i.e., R -curve behaviour. Consistent with this suggestion was the observation that sometimes the primary crack was arrested before final failure of the composite (Fig. 9).

The toughness of the cold formed monolithic material was $1.39 \pm 0.19 \text{ MPam}^{1/2}$ materials which is similar to the bottom of the range measured for the hot pressed monolithic materials. The increase in toughness on incorporating a reinforcement (Fig. 10) produced values that compared favourably with the those of the best hot pressed composites.

Due to the presence of a high density of large ($\sim 10 \mu\text{m}$) pores in the cold formed monolithic material its strength was only 82 MPa. The adverse effect of the pores was ameliorated by the ductile reinforcement and strength values comparable to the best obtained via the hot pressing route were recorded (Fig. 10). The mechanical properties of the cold formed composites were encouraging and hence this may be the preferable processing route rather than the more expensive hot pressing.

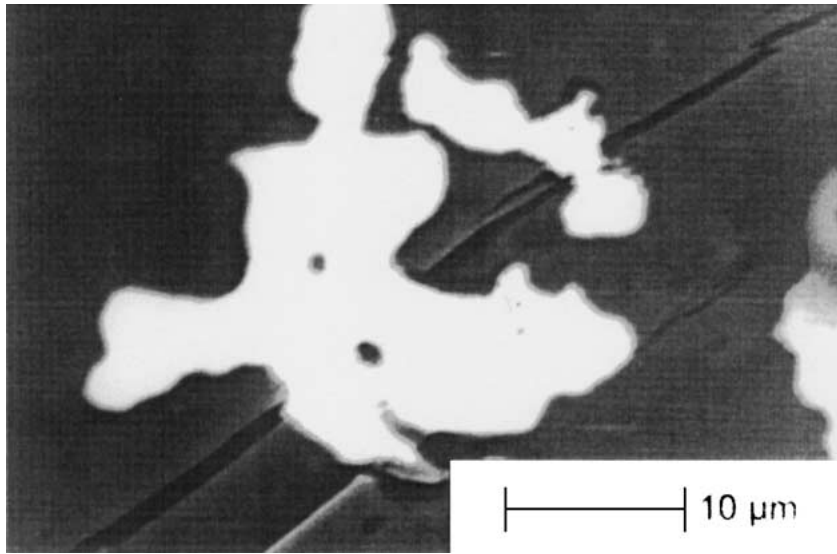


Figure 7 Backscattered electron image showing cracks propagating towards silver particles and the onset of debonding (CP1 : 2.5ss/925).

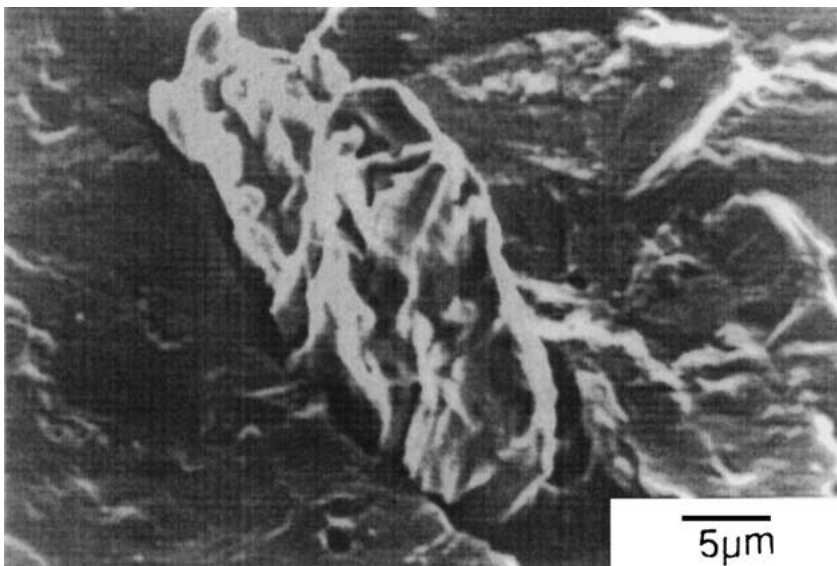


Figure 8 Secondary electron image of the fracture surface showing a heavily deformed and fractured silver particle (CP1-10/1000).

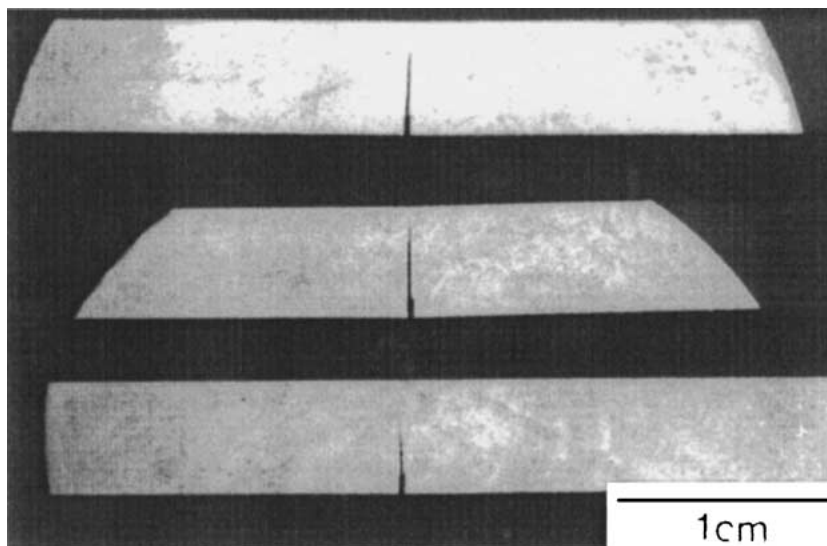


Figure 9 Photographs showing examples of fracture toughness specimens where the crack has been arrested within the specimen (CP1-10/1000).

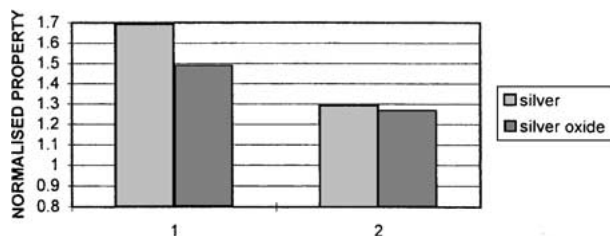


Figure 10 Normalised strength (1) and toughness (2) for cold formed, sintered and crystallised composites with silver and silver oxide reinforcement precursors.

4. Conclusions

1. Apoceram glass-ceramics reinforced with 10vol% silver have been successfully produced by two routes: (i) hot pressing and (ii) cold pressing, isostatic pressing followed by sintering and crystallisation. There was no difference in the microstructure of the matrices other than the presence of large ($\sim 10 \mu\text{m}$) pores in the cold formed materials. The matrices were free from microcracks and no reaction was observed between the matrix and the silver particles. The latter were obtained by mixing either silver or silver oxide with the parent glass; agglomeration was more marked when the oxide was used.

2. The strength and toughness of the hot pressed composites processed at 850–900°C inclusive were slightly better than the corresponding monolithic materials. More impressive was the improvement in the mechanical properties on the incorporation of silver particles in cold formed material, which resulted in the properties of the hot and cold formed composites being similar.

The observation of crack arrest and extensive deformation of the silver particles suggested that these composites might exhibit strong *R*-curve behaviour.

3. The results indicate that future development of these composites is unlikely to involve silver oxide as a precursor for the ductile reinforcement and should concentrate on the less expensive cold forming process route.

Acknowledgements

Two of the authors (EC and BAT) gratefully acknowledge the award of EPSRC studentships.

References

1. D. E. WILLIAMS (ed.), "Definitions in Biomaterials" (Elsevier, 1987).
2. L. L. HENCH and H. A. PASCHALL, *J. Biomed. Mater. Res. Symp.* **4** (1973) 25.
3. L. L. HENCH, R. J. SPLINTER, W. C. ALLEN and T. K. GREENLEE, *J. Biomed. Mater. Res.* **2** (1972) 117.

4. H. BROMER, E. PFEIL and H. H. KAS, German Patent no. 2326 100 (1973).
5. H. BROMER, K. DEUTSCHER, B. BLENKE, E. PFEIL and V. STRUNZ, "Science of Ceramics," Vol. 9, Nederlandse Keramische Vereniging (1977) p. 219.
6. H. H. KAS, German Patent no. 2349 859 (1975).
7. T. KOKUBO, M. SHIGEMATSU, Y. NAGASHIMA, M. TASHIRO, T. M. NAKAMURA, T. YAMAMURO and S. HIGASHI, *Bull. Inst. Chem. Res. Kyoto University* **60** (1982) 260.
8. T. KOKUBO, S. ITO, S. SAKKA and T. YAMAMURO, *J. Mater. Sci.* **21** (1986) 536.
9. T. KOKUBO, S. ITO, M. SHIGEMATSU, S. SAKKA and T. YAMAMURO, *Ibid.* **20** (1985) 2001.
10. P. R. CARPENTER, M. CAMBELL, R. D. RAWLINGS and P. S. ROGERS, *J. Mater. Sci. Lett.* **5** (1986) 1309.
11. R. D. RAWLINGS, P. S. ROGERS and P. M. STOKES, "High Tech Ceramics," edited by P. Vincenzini (Elsevier Science, Amsterdam, 1987) p. 73.
12. H. ALANYALI, R. D. RAWLINGS and P. S. ROGERS, *Brit. Ceram. Trans.* **97** (1998) 240.
13. T. B. TROCZYNSKI and P. S. NICHOLSON, *J. Amer. Ceram. Soc.* **73** (1990) 164.
14. T. B. TROCZYNSKI, P. S. NICHOLSON and C. E. RUCKER, *ibid.* **71** (1988) C276.
15. P. DUCHEYNE and H. H. HENCH, *J. Mater. Sci.* **17** (1982) 595.
16. T. B. TROCZYNSKI and P. S. NICHOLSON, *J. Amer. Ceram. Soc.* **74** (1991) 1803.
17. T. KASUGA, K. NAKAJIMA, T. UNO and M. YOSHIDA, *ibid.* **75** (1992) 1103.
18. CH. MULLAE-MAI, H.-J. SCHMITZ, V. TRUNZ, G. FUHRMANN, TH. FRITZ and U. M. GROSS, *J. Biomed. Mat. Res.* **23** (1989) 1149.
19. F. PERNOT and R. ROGIER, *J. Mater. Sci.* **27** (1992) 2914.
20. *Idem.*, *ibid.* **28** (1993) 6676.
21. B. A. TAYLOR, R. D. RAWLINGS and P. S. ROGERS, in "Bioceramics," Vol. 7, edited by O. H. Andersson and A. Yli-Urpo (Butterworth-Heinemann, 1994) p. 255.
22. E. CLAXTON, R. D. RAWLINGS and P. S. ROGERS, *Brit. Ceram. Proc. No. 55*, edited by D. P. Thompson and H. Mandal (Inst. Mater., 1996) p. 101.
23. *Idem.*, in Proc. 7th Europ. Conf. on Composite Materials (Woodhead Publishing, Cambridge, 1996) Vol. 2, p. 461.
24. R. BALZER, K.-L. CHOY and R. D. RAWLINGS, *J. Eur. Ceram. Soc.* **20** (2000) 2199.
25. J. E. SRAWLEY, *Int. J. Fracture* **12** (1976) 475.
26. R. D. RAWLINGS and P. S. SANDHU, unpublished work.
27. R. ROGIER and F. PERNOT, *J. Mater. Sci.* **26** (1991) 5664.
28. V. D. KRSTIC and M. D. VLAJIC, *Acta. Metall.* **31** (1983) 139.
29. J. SELSING, *J. Amer. Ceram. Soc.* **44** (1961) 419.
30. T. KOKUBO, *J. Non-Cryst. Sol.* **120** (1990) 138.
31. M. F. ASHBY, F. J. BLUNT and M. BANNISTER, *Acta. Metal.* **37** (1989) 1847.

Received 14 May 2001

and accepted 5 March 2002